Rover Operations for Subsurface Mining on the Moon

Ellery A*, Schwarz M, Molina Cabreira P, Lynch B, Frazier C, Mack A
*Canada Research Professor
Centre for Self-Replication Research (CESER)
Department of Mechanical & Aerospace Engineering
Carleton University
Ottawa, CANADA

Rationale for Subsurface Mining

- **Objective**: Industrialise the Moon using in-situ resources minimising Earth supply chain
- Moon has not experienced aqueous processes of weathering and erosion that yield geographical concentrations of orebodies
- Moon has a relatively simple geology comprising a few common rock-forming minerals, e.g. **plagioclase feldspars** (esp anorthite) – **pyroxene** - **olivine** – **ilmenite**
- Our **DEMANDITE** concept maps functional material requirements with available lunar resources
- **10 basic materials** can supply full functionality for all the subsystems of a generic robotic spacecraft
- To determine the **proportions that constitute the demandite**, we use a variation on a standard spacecraft model with a dry mass allocation of 100%

Functionality (mass fraction)	Lunar-Derived Material
Tensile structures (25%)	Wrought iron Aluminium
Compressive structures (+50%)	Cast iron Regolith + binder
Elastic structures (trace)	Steel springs/flexures Silicone elastomers
Hard structures (3%)	Alumina
Thermal conductor straps (1%)	Fernico (e.g. kovar) Nickel Aluminum
Thermal radiators (3%)	Aluminium
Thermal insulation (3%)	Glass (SiO_2 fibre) Ceramics such as SiO_2
High thermal tolerance (4%)	Tungsten Alumina
Electrical conduction wire (7%)	Aluminium Fernico (e.g. kovar) Nickel
Electrical insulation (1%)	Glass fibre Ceramics (SiO_2, $Al_2O_3$and TiO_2) Silicone plastics Silicon steel for motors
Active electronics devices (vacuum tubes) (12%)	Kovar Nickel Tungsten Fused silica glass
Magnetic materials for actuators (5%)	Ferrite Silicon steel Permalloy
Sensory transducers (5%)	Resistance wire Quartz Selenium
Optical structures (11%)	Polished nickel/aluminium Fused silica glass lenses
Lubricants (trace)	Silicone oils Water
Power system (20%)	Fresnel lens + thermionic conversion Flywheels
Combustible fuels (+250%)	Oxygen Hydrogen

Lunar Industrial Ecology

Lunar Ilmenite

$Fe^0 + H_2O \rightarrow$ ferrofluidic sealing

$FeTiO_3 + H_2 \rightarrow \mathbf{TiO_2} + H_2O + \mathbf{Fe}$

$2H_2O \rightarrow 2H_2 + O_2$

$2Fe + 1.5O_2 \rightarrow Fe_2O_3/Fe_2O_3.CoO$ - ferrite magnets

Nickel-iron meteorites

$Fe(CO)_5 \leftrightarrow 5CO + Fe$ (175°C/100 bar) →

$Ni(CO)_4 \leftrightarrow 4CO + Ni$ (55°C/1 bar) →

$Co_2(CO)_8 \leftrightarrow 8CO + 2Co$ (150°C/35 bar) →

S catalyst

Alloy	Ni	Co	Si	C	W
Tool steel				2%	9-18%
Electrical steel			3%		
Permalloy	80%				
Kovar	29%	17%	0.2%	0.01%	

$4FeS + 7O_2 \rightarrow \mathbf{2Fe_2O_3} + 4SO_2$

(Troilite) $SO_2 + H_2S \rightarrow 3S + H_2O$

$FeSe + Na_2CO_3 + 1.5O_2 \rightarrow \mathbf{FeO} + Na_2SeO_3 + CO_2$

KNO_3 catalyst $Na_2SeO_3 + H_2SO_4 \rightarrow Na_2O + H_2SO_4 + Se \rightarrow$ photosensitive Se

W inclusions – high density of 19.3 → cathodic material

Olivine

$Mg_2SiO_4 + 2CH_4 \rightarrow 2CO + H_2 + \mathbf{2MgO} + Si$ at 2000°C → 3D Shaping binder

$MgO + HCl \rightarrow MgCl_2 + H_2O$ → 3D Shaping binder

$CO + 0.5\ O_2 \rightarrow CO_2$

$CO_2 + 4H_2 \rightarrow CH_4 + 2H_2O$ at 300°C (Sabatier reaction) $\rightarrow CH_4 \rightarrow C + 2H_2$ at 1400°C for steel

Ni catalyst

Lunar Anorthite

$CaAl_2SiO_8 + 4C \rightarrow CO + \mathbf{CaO} + \mathbf{Al_2O_3} + 2Si$ at 1650°C → CaO cathode coatings

$CaO + H_2O \rightarrow Ca(OH)_2$

$Ca(OH)_2 + CO_2 \rightarrow CaCO_3 + H_2O$

$CaAl_2SiO_8 + 5HCl + H_2O \rightarrow CaCl_2 + 2AlCl_3.6H_2O + \mathbf{SiO_2}$ → fused silica glass + metalysis electrolyte

$AlCl_3.6H_2O \rightarrow Al(OH)_3 + 3HCl + H_2O$ at 100°C

$Al(OH)_3 \rightarrow \mathbf{Al_2O_3} + 3H_2O$ at 400°C $\rightarrow 2Al + Fe_2O_3 \rightarrow 2Fe + Al_2O_3$ (thermite)

AlNiCo hard magnets

Al solar sail

Lunar Volatiles

$CH_4 + H_2 \xrightarrow[\text{Ni catalyst}]{850°C} CO + 3H_2 \xrightarrow[Al_2O_3]{250°C} CH_3OH$

$CH_3OH + HCl \xrightarrow[Al_2O_3]{350°C} CH_3Cl + H_2O$

$CH_3Cl + Si \xrightarrow{370°C} (CH_3)_2SiCl_2 \xrightarrow{+nH_2O} ((CH_3)_2SiO)_n + 2nHCl$ → silicone plastics/oils

$3NO + H_2O \rightarrow 2HNO_3 + NO$

$2SO_2 + O_2 \leftrightarrow 2SO_3$ (low temp)

$SO_3 + H_2O \rightarrow H_2SO_4$

Salt of the Earth

$NaCl + CaCO_3 \rightarrow Na_2CO_3 + CaCl_2$ → metalysis electrolyte

$Na_2CO_3 + SiO_2(i) \xleftrightarrow{350°C/150\ bar} Na_2SiO_3 + CO_2$ → piezoelectric quartz

$NaCl + HNO_3 \rightarrow HCl + NaNO_3$

Lunar Orthoclase

$2KAlSi_3O_8 + HCl + 9H_2O \rightarrow H_4Al_2Si_2O_9 + 2KCl + SiO_2 + H_2O$

Kaolinite $KCl + NaNO_3 \rightarrow NaCl + KNO_3$

Iron Metallurgy on the Moon

- **Hydrogen reduction of ilmenite** at ~1000ºC creates oxygen, iron and rutile
  $FeTiO_3 + H_2 \rightarrow Fe + TiO_2 + H_2O$ and $2H_2O \rightarrow 2H_2 + O_2$
- Fe separated from TiO_2 by liquation at 1600ºC
- **Wrought iron** is tough & malleable for tensile structures
- **Cast iron** (~2-4% **C** + 1-2% **Si**) is more brittle for compressive structures (e.g. Iron Bridge for 200+y)
- **Tool steel** (<2% **C** + 9-18% **W**) for cutting tools, e.g. milling head (substitutable with **silumin**)
- **Invar** (64% Fe, 36% **Ni**) and **inovco** (62.5% Fe,33% **Ni**,4.5% **Co**) for high precision mechanisms with low CTE
- **Silicon (electrical) steel/ferrite** (up to 3% **Si** and 97% Fe) for electromagnets and motor cores - 3% Si increases electrical resistivity by 4 x
- **Kovar** (53.5% Fe, 29% **Ni**, 17% **Co**, 0.3% Mn, 0.2% **Si** and <0.01% **C -** Mn reduces brittleness) – fernico alloy for high temperature electrical/thermal conductors
- **Cryogenic** fernico (to -180ºC) trades more (31%) **Ni** for less (15%) Co
- **Permalloy** (20% Fe + 80% **Ni**) provides magnetic shielding with μ_r~10^5 H/m (replace 5% Ni with Mo gives supermalloy with μ_r~10^6 H/m) for electron guns

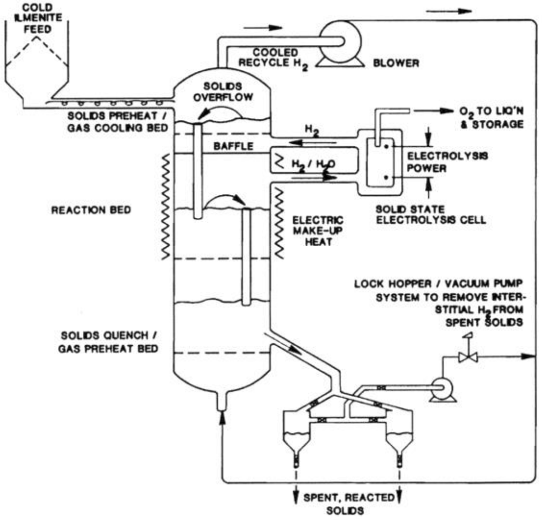

Asteroidal Sources on the Moon

- We need to source Tungsten, Nickel, Cobalt and Selenium for our alloy range
- Shoemaker crater scaling formula relates transient impact crater diameter to impact energy:
- $D = 0.01436\left(E\frac{\rho_{imp}}{\rho_{tgt}}\right)^{\frac{1}{3.4}}\left(\frac{g_{Earth}}{g_{tgt}}\right)^{\frac{1}{6}}(sin\alpha)^{2/3}$
- For low α, D is diminished and presumably penetration depth
- This determines mass of ejecta $m_{ejecta} = \rho V = \frac{\pi}{6}D^3\rho^2A$ and so the degree of concentration of asteroid material in the ejecta
- Simulations by various groups suggest that **there should be concentrations of asteroidal metal** deposited at shallow depths for shallow angle impacts
- **Asteroidal NiFe** resources are expected to be located at shallow-angle impact craters
- Some 25% lunar impactor material survives impact at or near surface of crater (670 crater >10 km diameter)
- **Mascons may** indicate location of **NiFe** meteorite ore concentrations, e.g. northern rim of SPA crater

Tunicose Ores from NiFe Meteorites

- M-type asteroid-derived meteoritic NiFe dominated by kamacite/taenite (**88% Fe/10%** Ni alloys) - typically **contaminated with 0.5% Co**
- Ni and Co are common catalysts and alloying material – Ni for heat tolerance and Co for corrosion-resistance in steels
- Special alloys, e.g. **AlNiCo** permanent magnets
- NiFe alloys **enriched in W microparticle inclusions** which can be crushed and separated out through several processes (W has high density of 19.3 and high melting temperature of 3422^{o}C)
- **S/Se ratio** in meteorites is **~2450** with **S~5%** content
- Se may be sourced as **FeS (troilite)-substituted FeSe ~1/2450** as grains in NiFe asteroid alloy
- Iron selenide may be smelted with soda $\mathbf{Na_2}CO_3$ and saltpetre $\mathbf{KNO_3}$ catalyst:

$$FeSe + Na_2CO_3 + 1.5O_2 \rightarrow FeO + Na_2SeO_3 + CO_2$$

- Selenite Na_2SeO_3 is acidified with H_2SO_4 (recycled) to yield selenous acid (H_2SeO_3) from which **Se may be precipitated**:

$$H_2SeO_3 + 2SO_2 + H_2O \rightarrow Se + 2H_2SO_4$$

Se is recovered with sulphuric acid recycled

Extraction of Ni-Co

- Ni and Co have similar electrical conductivities
- Carbonyl (Mond) volatilises powdered NiFeCo alloy into transition metal carbonyls $M_x(CO)_y$
- This yields 99.99% purity elemental metal with Fe, Ni and Co separated by **fractional distillation**

Physical Conditions (LHS)	Carbonyl Process	Physical Conditions (RHS)
175-230°C and 60 bar	$Ni + 4CO \leftrightarrow Ni(CO)_4$	50-60°C
200°C	$Fe + 5CO \leftrightarrow Fe(CO)_5$	105°C and 100-300 bar
80-120°C and 95-110 bar	$2Co + 8CO \leftrightarrow Co_2(CO)_8$	55°C and 35 bar

- Carbonyls decompose thermally into high purity metals using S catalyst
- **S** catalyst recovered at 750-1100°C from troilite (**FeS**) in meteoritic inclusions, lunar regolith (~1%), or lunar volatiles (SO_2 and H_2S gases)

$4FeS + 7O_2 \rightarrow 2Fe_2O_3 + 4SO_2$ and $SO_2 + H_2S \rightarrow 3S + H_2O$

- Carbonyl process is suited to low-temperature **CVD** of Fe, Ni and Co coatings

Kapvik Rover Chassis

- There are many suitable mobility systems for lunar terrain
- For Kapvik, we adopted the six-wheeled rocker-bogie system as the reference chassis due to its flight heritage
- It was extensively field tested at the CSA Mars Yard
- With a modular chassis, Kapvik could accommodate different chassis modules exchangeable within 3 minutes
- We designed a Kapvik modular elastic loop mobility system for high traction on rugged terrains at the lunar poles

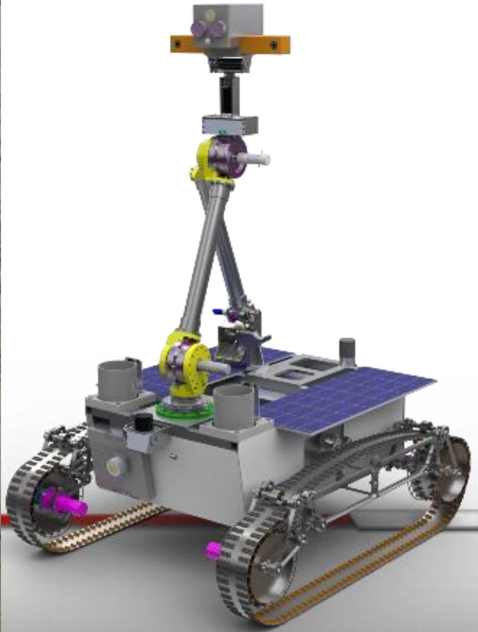

Abseiling Kapvik

- There are natural subsurface mines with potential water ice deposits more readily accessible than shadowed craters at the poles
- Skylights are partially collapsed roofs to subsurface lava tubes
- Examples include three skylights at Mare Igenii, Mare Tranquillitatis and Marius Hills with diameters ~50-100 m and depths ~40-100 m
- Kapvik can abseil down steep crater cliffs using tethers
  - it adopted a freewheeling descent with descent controlled by tether deployment (unlike cliffbot)
- Winching from a skylight into a lava tube would be more challenging due to stability vulnerabilities

Rover Prospecting

- Prospecting for lunar in-situ resources is required to determine **stripping ratios of waste to ore** to determine how to recover metals, glasses and ceramics from lunar minerals
- We have conducted rover-based trials using a Pioneer robot at the **open quarry asbestos Jeffrey Mine, Quebec** to search for serpentine deposits
- This mainly to test CSA ExDOC software control system
- Our end-to-end **32 kg Kapvik** (Inuit for wolverine) micro-rover has been a testbed for exploring several issues relevant to **advanced ISRU activities on the Moon** especially mining

- It is expected that low angle impacts may result in asteroidal material survival on or beneath the lunar surface, i.e. ~600 crater candidates
- Non-indigenous **Ni-Fe-Co-W-Se may be sourced** from these regions
- There may be indications from **local magnetic anomalies**

Geomagnetic Survey

- Surveying is essential to find specific in-situ resources
- We are specifically interested in detecting local surface magnetic indications of potential **near surface NiFe asteriodal ores** implanted by low-angle impactors
- Kapvik has been fitted with a **boom-mounted magnetometer** instrument to field test ground magnetic survey by rover at Carleton University campus

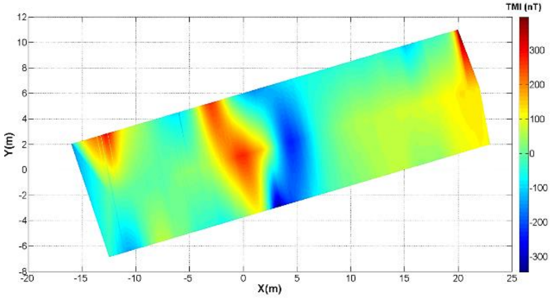

- It successfully detected an underground storm sewer and a local fault, demonstrating the principle of rover-mounted magnetometry
- Similar surveying methods may be applied to **ferromagnetic detection**

Lunar Mines

- Subsurface incidence and distribution of orebodies is unknown – there may be large and/or small orebodies
- There are several constraints we can impose on lunar mines for asteroid ores:
  - **lunar mines will be smalll**er in scale than terrestrial mines
  - **large-scale highwall mining machines are discarded** due to prohibitive costs
  - **spiral strip mining is more efficient** than rectilinear parallel strips
  - **open-pit mining** wastes effort in **removal of large amounts of overburden**
- **Underground mining** is characterised by their wall and roof supports – room-and-pillar, stope-and-pillar, cut-and-fill stoping, sublevel caving, etc
  - mechanised cut-and-fill mining may be most suitable
  - automated load-hail-dumper vehicles are essential in all mine types
- **Adaptability to rugged sloping terrain** will be crucial.

Geotechnic Survey by Rover

- Terramechanics metric, drawbar pull DP=H-R where H=soil thrust derived from Mohr-Coulomb relation $\tau = c + \sigma tan\phi$, τ=soil shear, c=soil cohesion, φ=soil friction angle, σ=soil stress, R=soil resistance dominated by compaction resistance due to sinkage $z = (\sigma/k)^{1/n}$, k=pressure-sinkage coefficient, n=soil exponent
- Sinkage may be estimated from wheel pressure σ from wheel loads measured by load sensors integrated above each wheel station of Kapvik
- Neural network model yields soil cohesion and friction angle estimates – tactile sensing of geotechnic data for lunar bases as the rover traverses

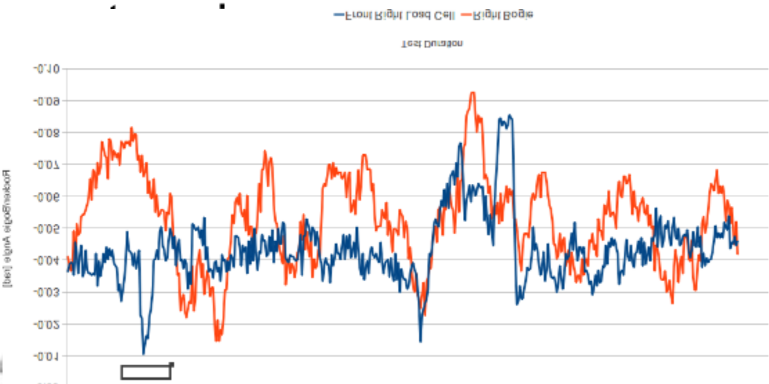

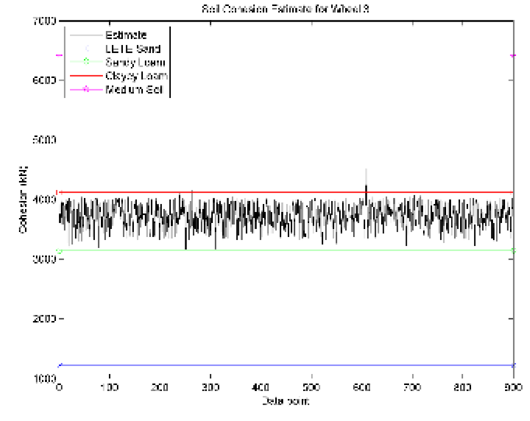

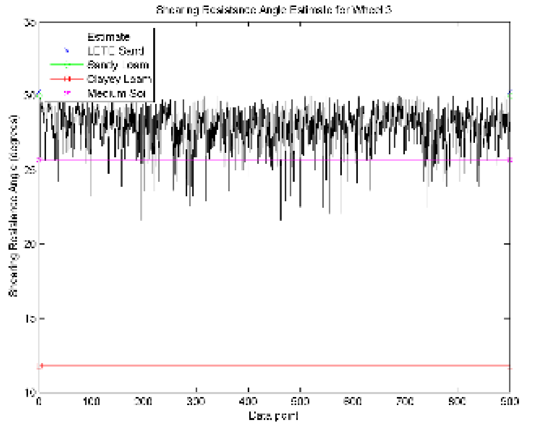

Rover Slippage

- **Slip can also be estimated** while traversing terrain as a sharp shift in soil cohesion

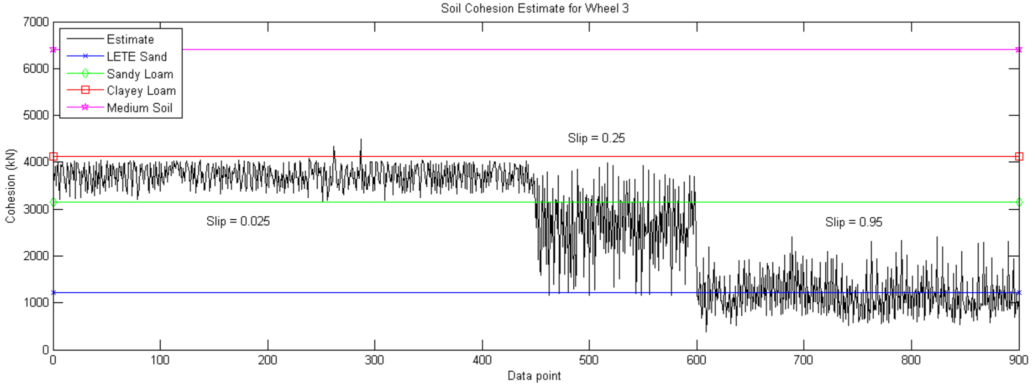

- We simulated slip over Martian terrain using the Lindmann-Voorhees polynomial slip model – we trained a neural network model using EKF learning rule to predict slip and compensate for it – perhaps a sigmoidal model offers insights into slip

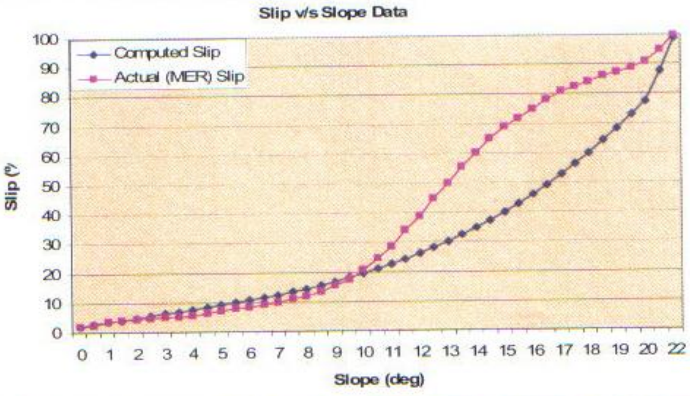

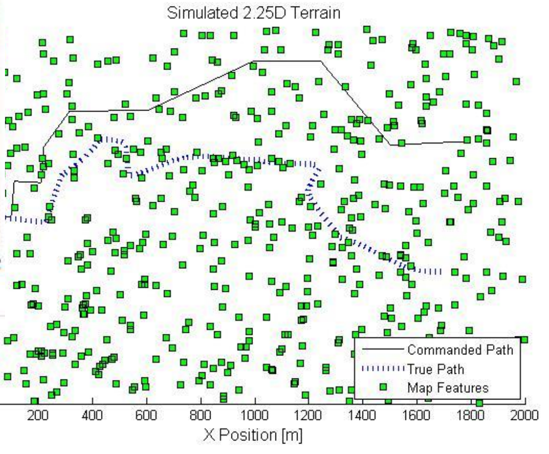

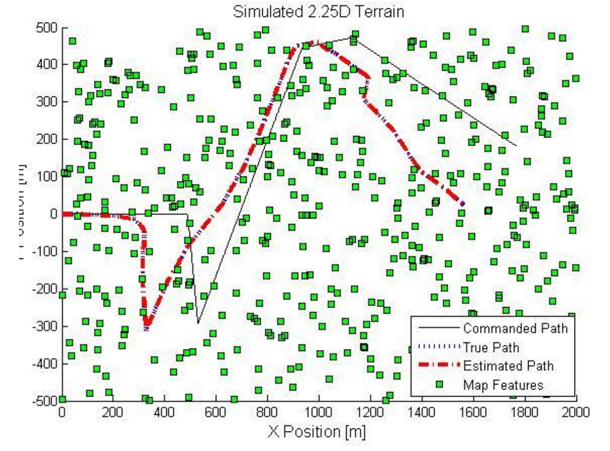

Kapvik Hoe! Regolith Acquisition

- Kapvik is configured similarly to a JCB with a 4 degree-of-freedom articulated arm at the end of which is a soil scoop

- From Reece earth-moving equation, maximum total tool digging force applied by Kapvik's weight on the Moon limits digging depth to 17 cm

Parameter	**Symbol**	**Value**
Soil density	ρ	1520 kg/m^3
Soil cohesion	C	170 Pa
Soil friction angle	Φ	35^o
Tool width	b	0.20 m
Tool cut height	h	
Tool rake angle of approach	α	80^o
Soil shear plane angle	β	$45+\varphi/2$
Soil-blade friction angle	δ	$\varphi/3$

Simultaneous Localisation & Mapping

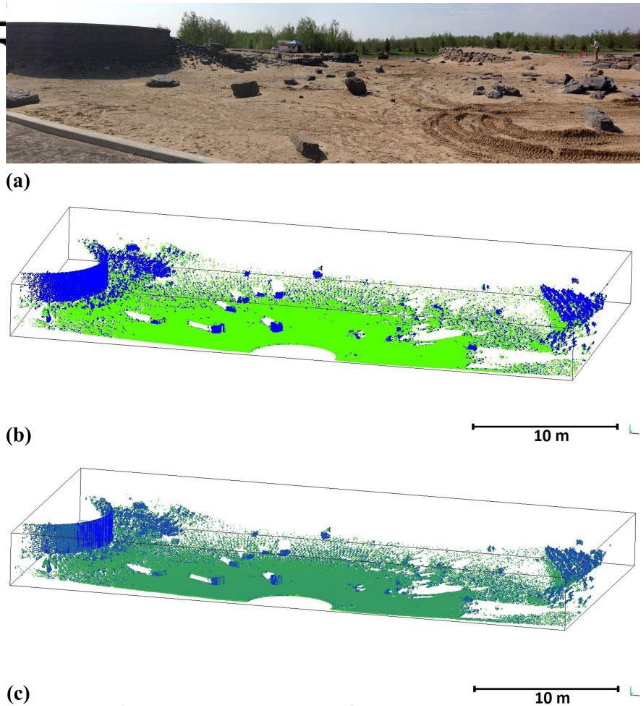

- Kapvik's primary navigation instrument is a LIDAR scanner for 3D mapping of the local environment
- AutoNav is based on SLAM in which a rover locates itself within a map of its environment characterised by landmarks represented as 3D point clouds
- Map is occupancy grid of cells labelled with probabilistic classifications of traversibility
- We used neural network classifier of terrain trained by EKF learning rule of the form $w_{t+1} = w_t + K_t\left(y_t^d - h(x_t)\right)$ where $K_t = P_t H_t\left(1/\eta + H_t^T P_t H_t\right)^{-1}$=Kalman gain, $\eta = \left(H_t P_t H_t^T + R_t\right)^{-1} P_t$=learning rate
  - EKF exploits more info than BP
- Kapvik implemented several SLAM algorithms on two Xiphos Q5 FPGA platforms

Computation of Visual Mapbuilding

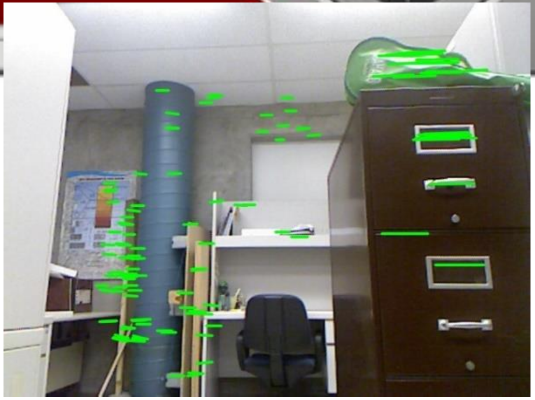

- SLAM may be implemented using visual mapbuilding
- We used an indoor environment to emulate cluttered obstacles enclosed in confining walls and doorways
- Kinect camera with RGB-D capabilities was mounted onto a Husky rover
- For visual odometry, we compared feature detection algorithms
  – SIFT and SURF yielded similar computational overhead
  - BRISK and ORB offer higher computational efficiency
  - BRISK was slightly faster than ORB

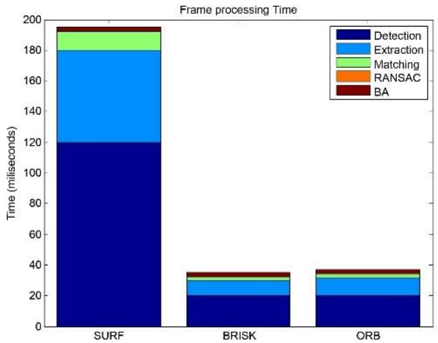

- We simulated the roundtrip Freidberg trajectory using BRISK to test loop closure → Recalibration for multiple traverses through mining tunnel

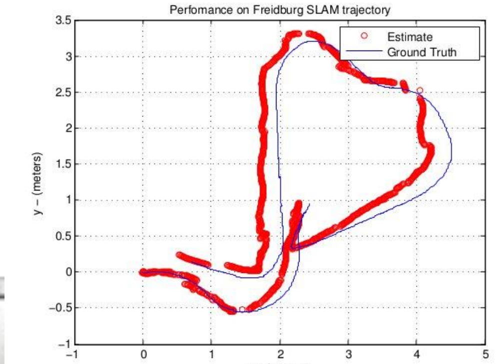

Rover Pan-Cam Control

- Kapvik is configured with a Point Grey Bumblebee colour stereo camera mounted onto a pan/tilt unit at the elbow of 4 DOF arm
- To search for targets during traverse, pan-tilt unit allows camera to track targets using an artificial "vestibular-ocular reflex"
- We replaced gyroscopic feedback with pan-tilt joint measurement feedback augmented by dynamic feedforward neural network model (emulating cerebellar function)

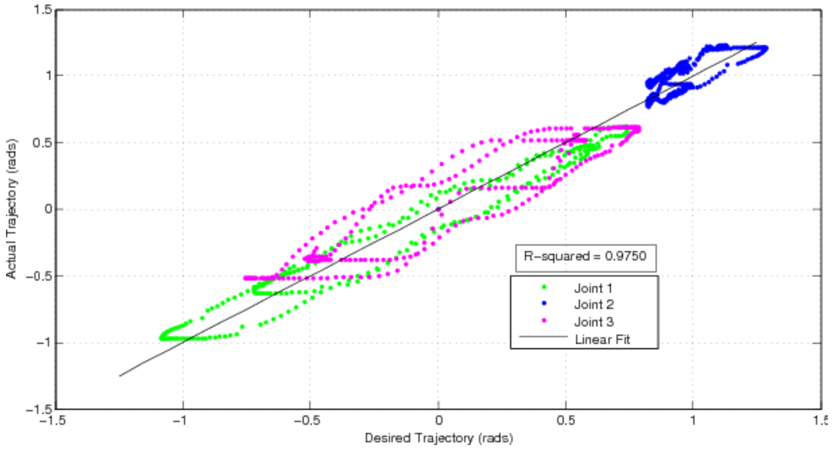

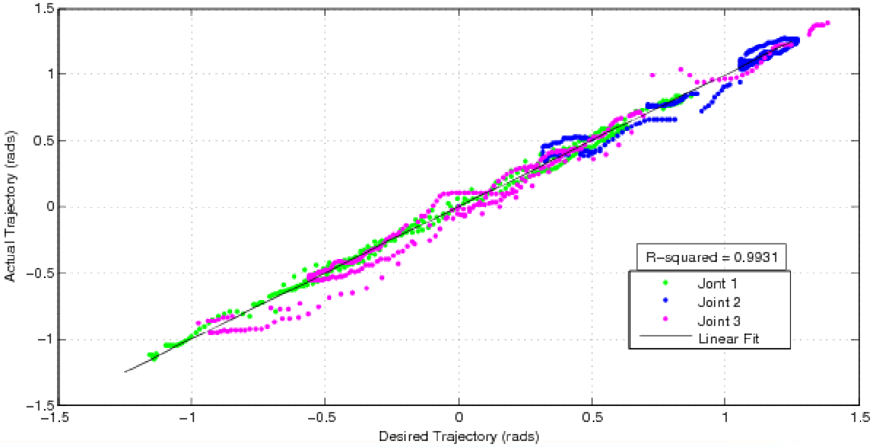

Path Planning

- We investigated potential fields for path planning and execution
- Potential fields implement sum o attractive (goal) and repulsive forces (obstacles) to generate traverse gradient along potential minimum path while avoiding obstacles: $F=F_{gl} + \Sigma F_{obs}$
- We simulated the Fajen-Warren polar potential field through Mars rock distributions but it failed through highly cluttered MPF rock field

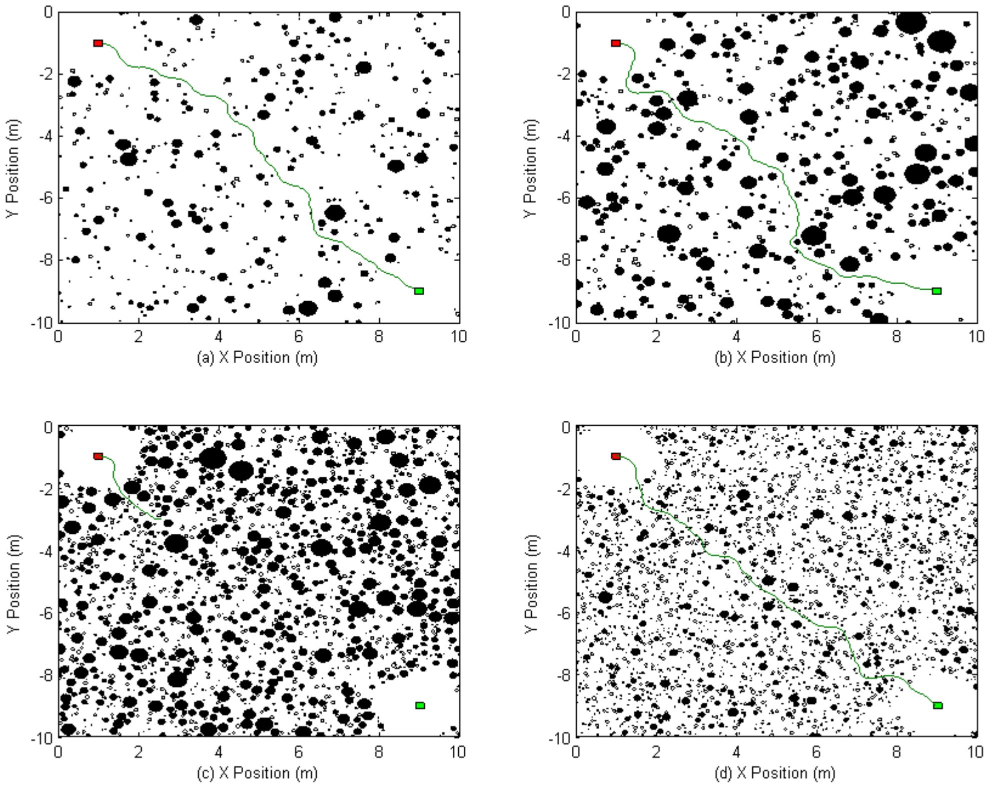

Path Planning 2

- We require a more robust strategy for dealing with cluttered environments, especially narrow passageways (characteristic of underground mines)
- We added risk and tangential forces to shape the potential field
- Risk force applies an exponential velocity factor to obstacle force to slow down close approaches

  $F_{rsk} = -\varepsilon k_{rsk} F_{obs}$ and $\tau_{rsk} = -\varepsilon k_{rsk} \tau_{obs}$ where $\varepsilon = exp\left(-k_{dcy} v_x\right)$, k_{dcy}=const
- Tangential force applies an exponential velocity factor that generates a bias force when rover slows to eject from local minima

  $F_{tgl} = \varepsilon \gamma k_{tgl} R(\pi/2) F_{obs}$ and $\tau_{tgl} = r_f \times F_{tgl}$ where k_{tgt}=const
- These tailoring forces are effective in coping with cluttered environments
- Potential field is suitable for multi-rover coordination

“Field” tests of Potential Field

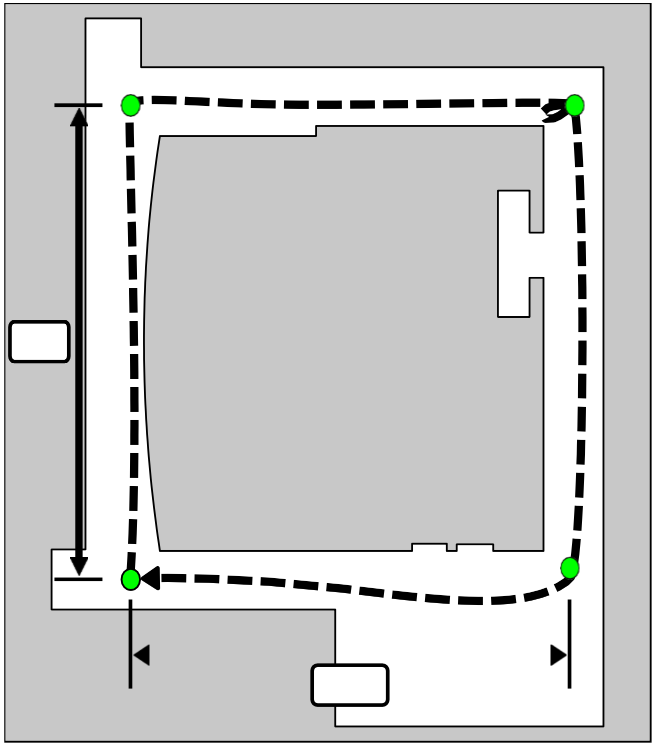

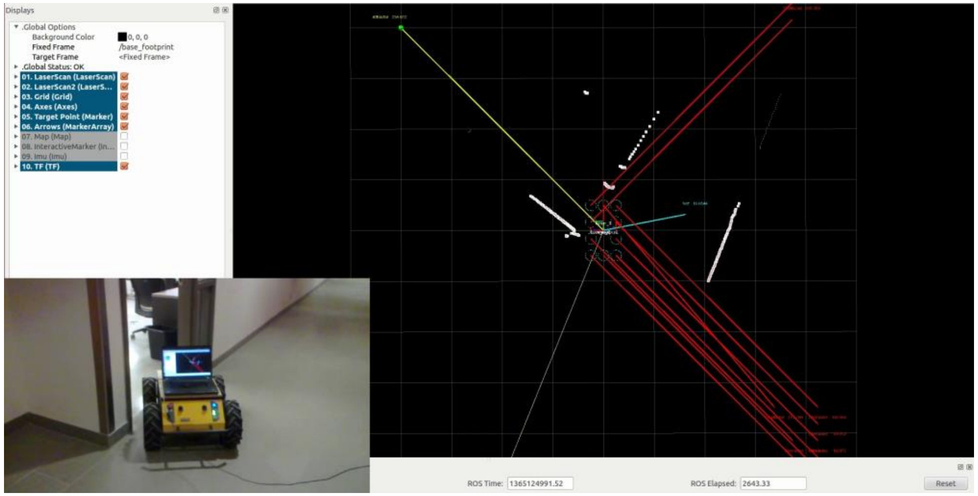

Displays

- .Global Options
  - Background Color: 0, 0, 0
  - Fixed Frame: /base_footprint
  - Target Frame: <Fixed Frame>
- .Global Status: OK
- 01. LaserScan (LaserScan) ☑
- 02. LaserScan2 (LaserS... ☑
- 03. Grid (Grid) ☑
- 04. Axes (Axes) ☑
- 05. Target Point (Marker) ☑
- 06. Arrows (MarkerArray) ☑
- 07. Map (Map) ☐
- 08. InteractiveMarker (In... ☐
- 09. Imu (Imu) ☐
- 10. TF (TF) ☑

ROS Time: 1365124991.52

ROS Elapsed: 2643.33

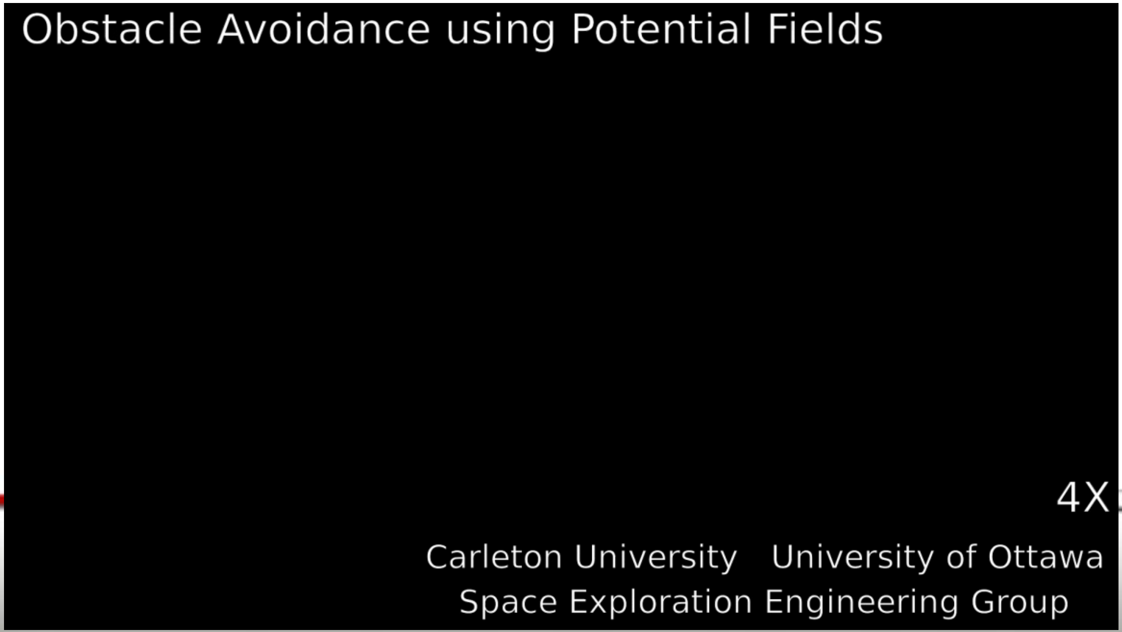

Obstacle Avoidance using Potential Fields

4X

Carleton University University of Ottawa
Space Exploration Engineering Group

Conclusions

- We have explored some aspects of subsurface mining on the Moon to acquire Ni-Co-W-Se sources from buried NiFe meteorite material
- Subsurface mining to access such resources are essential to realise robust industrialisation of the Moon